

Grain boundary diffusion coefficients in gold–nickel thin films

Ahmed M. Abdul-Lettif*

Physics Department, College of Science, Babylon University, Hilla, Iraq

Received 2 December 2002; Revised 3 March 2003; Accepted 7 March 2003

Polycrystalline gold–nickel thin films are deposited on silicon (111) wafers by evaporation in a vacuum of 2×10^{-6} mbar. Concentration profiles of heat-treated specimens are obtained by Auger electron depth profiling. The heat treatments are carried out in a vacuum furnace of 4×10^{-6} mbar in the temperature interval 473–773 K. The grain boundary diffusion coefficient is determined, using a modified Whipple model, to be $(3 \times 10^{-4} \text{ cm}^2 \text{ s}^{-1}) \exp(-0.94 \text{ eV kT}^{-1})$. It is concluded that interdiffusion in the investigated system is characterized by type B kinetics, and that grain boundary diffusion plays a dominant role in the mass transport process of such films. Copyright © 2003 John Wiley & Sons, Ltd.

KEYWORDS: grain boundary; diffusion coefficient; gold; nickel; AES

INTRODUCTION

One system routinely employed for packaging high-reliability microelectronic devices consists of gold-plated nickel. Nickel is used as an underplate instead of tin or lead for several reasons:

- (1) Unlike tin, nickel will not smear or transfer to and thus contaminate the gold button or gold plating on the contact point.
- (2) Much testing has demonstrated that a nickel underplate enhances the wear characteristics of gold.
- (3) The nickel barrier helps to reduce both the number and effect of pores, as opposed to plating gold directly.
- (4) Nickel acts as a diffusion barrier between the gold overlayer and the substrate.

Grain boundary diffusion often controls evaluation of the structure and properties of engineering materials at elevated temperatures. Short-circuit diffusion through grain boundaries is one of the main modes of device failure in microelectronics. Several analytical models and techniques have been proposed and applied^{1–6} for the analysis of grain boundary diffusion in thin specimens. In this work, a modified Whipple model¹ was used to determine grain boundary diffusion coefficients (D_b) in the temperature interval 473–773 K used in the fabrication processes of microelectronic devices. The aforementioned model needs to measure the concentration profiles of the diffusant materials. These profiles were obtained by Auger electron spectroscopy (AES) in combination with ion sputtering, as published previously⁷ by the author.

EXPERIMENTAL

Gold–nickel bilayer thin films were prepared on highly cleaned⁸ Si(111) wafers by the sequential evaporation of high-purity nickel (99.99%) and gold (99.99%) under an uninterrupted vacuum of 2×10^{-6} mbar. The thickness of each layer was 200 nm, with an average evaporation rate of 15 nm min^{-1} for the nickel layer and 13 nm min^{-1} for the gold layer. The substrates were maintained at 373 K during the deposition. After preparation, isothermal diffusion annealing was performed in a vacuum furnace of 4×10^{-6} mbar at constant temperature (473–773 K) for an annealing time of 5–180 min.

Concentration profiles were obtained using AES in combination with *in situ* Ar⁺ sputtering. The Auger system used was a SAM 660 scanning Auger microprobe manufactured by Perkin-Elmer and operated at the following specifications and conditions: for the primary electron beam the current was 500–600 nA, the incident energy was 5 keV and the beam width was $1 \mu\text{m}$ rastered across an area of $\sim 100 \times 100 \mu\text{m}^2$; for the Ar⁺ ion beam the voltage was 3 kV, the current was $0.8 \mu\text{A}$, the spot size was $800 \mu\text{m}$ scanned during sputtering in an area of $3 \times 3 \text{ mm}^2$, the basic vacuum in the analysis chamber was 3×10^{-10} mbar and during sputtering it was 2×10^{-8} mbar. The AES data were collected in the derivative mode using the 848 eV Ni peak and the 2024 eV Au peak. X-ray diffraction (XRD) analysis was achieved by a Philips PW 1710 automated diffractometer using monochromated Cu K α radiation of 1.5406 \AA wavelength.

RESULTS AND DISCUSSION

According to the modified Whipple model, the grain boundary diffusion coefficient (D_b) is best evaluated from the equation

$$D_b \delta = 0.661 \left(\frac{\partial \ln \bar{C}}{\partial y^{6/5}} \right)^{-5/3} \left(\frac{4D}{t} \right)^{1/2} \quad (1)$$

*Correspondence to: Ahmed M. Abdul-Lettif, Physics Department, College of Science, Babylon University, Hilla, Iraq.
E-mail: abdullettif1962@xiro.com
Contract/grant sponsor: Centre for Theoretical and Applied Physical Sciences, Yarmouk University, Jordan.

where δ denotes the effective grain boundary width ($\sim 0.5 \text{ nm}^3$), $(\partial \ln \bar{C} / \partial y^{6/5})$ is the slope of the plateau region of the average concentration (\bar{C}) profiles in the form of $\ln \bar{C}$ versus $y^{6/5}$ (y denotes the direction normal to the original interface), D denotes the intragranular diffusion coefficients (which have been determined⁹ for the same specimens to be 5.3×10^{-16} , 4.0×10^{-17} , 2.5×10^{-18} and $1.2 \times 10^{-19} \text{ cm}^2 \text{ s}^{-1}$ at 773, 673, 573 and 473 K, respectively) and t denotes the diffusion anneal time.

Figure 1 displays Wipple plots of $\ln \bar{C}$ versus $y^{6/5}$ for four specimens annealed at 773, 673, 573 and 473 K for 5, 20, 80 and 180 min, respectively. The atomic percentage was obtained by a computer program using an equation of the form¹⁰

$$C_i = \frac{I_i / A_{\text{rel}}^i}{\sum_{j=1}^n (I_j / A_{\text{rel}}^j)} \quad (2)$$

where C_i is the concentration of the i th component (in at.%), A_{rel} is the relative Auger yield, I_i is the measured peak-to-peak Auger intensity of component i and j is a running index over all the elements in the sample. The advances in improving the depth resolution made by Hofmann¹¹ were taken into account in the present analysis. Within $\sim 20 \text{ nm}$ of the interface, $\text{erfc}[y/2(Dt)^{1/2}]$ diffusion predominates. The apparent linearity of this part is due to the fact that $\ln [\text{erfc}(x)]$ is almost linear, with $x^{6/5}$ down to a concentration of 6%. The presence of grain boundary diffusion is evidenced by the breaks in the curves and the linear regions beyond 20 nm. The D_b values are determined by applying Eqn. (1) to the slopes of the latter regions (plateau regions): 3.2×10^{-10} , 1.7×10^{-11} , 9.6×10^{-13} and $3.7 \times 10^{-14} \text{ cm}^2 \text{ s}^{-1}$ at 773, 673, 573 and 473 K, respectively. The diffusion coefficient within the boundary exceeds the value within the grain by over five orders of magnitude, which means that $D_b \delta / 2D (Dt)^{1/2} \gg 1$, as required for Eqn. (1) to be valid. The D_b values are sufficiently large to explain the build-up of nickel at the gold surface for specimens annealed at 773 K for times as short as 5 min, i.e. the diffusion length $(2(D_b t)^{1/2} \sim 6200 \text{ nm})$ is larger than the gold film thickness (200 nm). The same analyses are valid for specimens annealed at 673, 573 and 473 K. The build-up of nickel at the gold surface may be attributed also to diffusion through a high defect density, such as the pinholes that were observed for these films.⁷

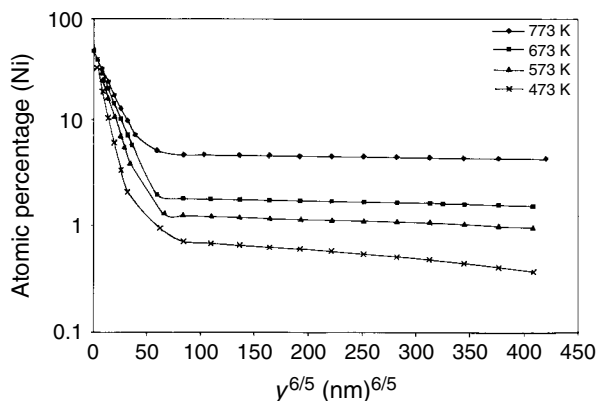


Figure 1. Wipple plot of nickel profiles in gold.

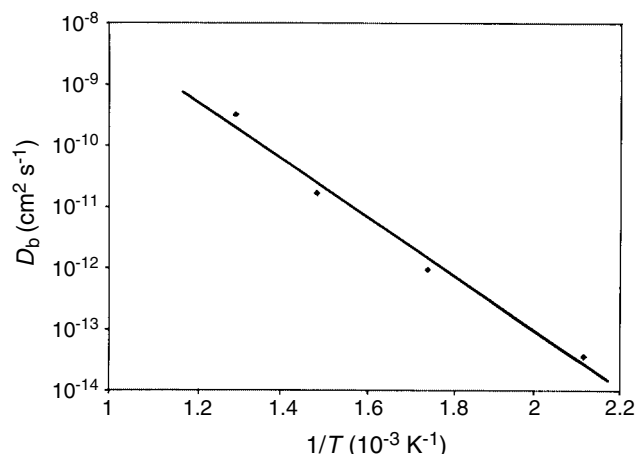


Figure 2. Grain boundary diffusion coefficient D_b as a function of $1/T$ for nickel in gold.

An Arrhenius plot of the D_b values versus $1/T$ is displayed in Fig. 2, wherein the equation of the curve is computed to be $D_b = (3 \times 10^{-4} \text{ cm}^2 \text{ s}^{-1}) \exp (-0.94 \text{ eV } kT^{-1})$. Because the error in determining D_b is constant or independent of temperature, only the pre-exponential term ($3 \times 10^{-4} \text{ cm}^2 \text{ s}^{-1}$) and not the activation energy (0.94 eV) should be sensitive to its effect. It is unusual to find the activation energy for D_b (0.94 eV) to be greater than that for D (0.87 eV).⁹ They are both, however, less than that for the bulk diffusion coefficient (1.8 eV) at high temperatures.¹²

Previous analysis suggests that interdiffusion in the gold–nickel thin-film system is characterized principally by type B kinetics.³ Here also diffusion along the boundary is accompanied by lateral leakage of the diffusant by volume diffusion, but the extent of this leakage is limited to distances much smaller than the grain size so that no overlapping of the diffusion fields from the neighbouring boundaries occurs and the boundaries can be considered as essentially isolated. This can be emphasized by comparing the volume diffusion lengths $(2(Dt)^{1/2})$ of 8, 4.4, 2.2 and 0.7 nm for the annealing conditions of the present work with the gold grain size of 55 nm determined from XRD analysis.¹³

It should be pointed out that the gold–nickel system is completely miscible at higher temperatures, as the phase diagram¹⁴ displays. However, there is a solubility limit of this system in the investigated temperature range. This solubility limit is nearly 4 wt.% (12.3 at.%) Ni in Au in the temperature range 473–873 K. The measured Ni atomic percentage in the investigation conditions is less than the solubility limit, and we predict that increasing the diffusion time would cause the diffusant Ni to exceed the solubility limit, which would alter the diffusion mechanisms in this system.

CONCLUSIONS

- (1) Interdiffusion in gold–nickel polycrystalline thin films is characterized principally by type B kinetics.
- (2) Grain boundaries play a dominant role in the mass transport process of such films.
- (3) The relatively large values of D_b are sufficient to account for the measured concentration profiles.

As temperatures in the range 473–773 K are routinely attained in processing protocols in the microelectronics industry, care must be taken to minimize intermetallic diffusion during device fabrication. Such diffusion could readily influence the reliability of specific devices. The present data suggest that diffusion can be minimized by preparing coarse-grained films, reducing the annealing temperature and time and avoiding oxidizing environments during thermal treatments.

Acknowledgements

This work was supported by the Centre for Theoretical and Applied Physical Sciences (CTAPS) in Yarmouk University (Jordan). The assistance of Dr Johann Vancea (Germany) is highly appreciated.

REFERENCES

1. Kaur I, Gust W. *Defect Diffus. Forum* 1989; **66–69**: 789.
2. Kaur I, Gust W. In *Diffusion in Solid Metals and Alloys*, Mehrer H (ed.). Springer-Verlag: Berlin, 1990; 630.
3. Kaur I, Mishin Y, Gust W. In *Fundamentals of Grain and Interphase Boundary Diffusion*. John Wiley: Chichester, 1995; 245.
4. Mishin Y, Herzig C. *Mater. Sci. Eng. A* 1999; **260**: 55.
5. Erdelyi Z, Girardeaux Ch, Langer GA, Daroczi L, Rolland A, Beke DL. *Appl. Surf. Sci.* 2000; **162/163**: 213.
6. Ostrovsky AS, Bokstein BS. *Appl. Surf. Sci.* 2001; **175**: 312.
7. Abdul-Lettif AM. *Surf. Interface Anal.* 2002; **33**: 306.
8. Uppal PN, Kroemer H. *J. Appl. Phys.* 1985; **58**: 2195.
9. Abdul-Lettif AM. *J. Mater. Sci.*
10. Hall PM, Morabito JM, Poate IM. *Thin Solid Films* 1976; **33**: 107.
11. Hofmann S. In *Progress in Surface Science*, vol. 36. Pergamon Press: Oxford, 1991; 35.
12. Murch GE, Bruff CM. In *Diffusion in Solid Metals and Alloys*, Mehrer H (ed.) Springer-Verlag: Berlin, 1990; 292.
13. Langford JI, Wilson AJC. *J. Appl. Crystallogr.* 1978; **11**: 102.
14. Smithells CJ. In *Metals Reference Book* (5th edn). Butterworths: London, 1976; 384.